High Efficiency Black Polymer Solar Cells
November 2012 Annual Report

PI: Dr. Franky So
External Collaborators: John Reynolds, Georgia Tech
Industry Partner: Sestar Technologies, LLC
Students: Cephas Small and Song Chen

Description: The objective of the proposed project is to synthesize broadly absorbing, black colored (PBLACK) polymers with especially high charge mobilities and to fabricate the highest performance polymer solar cells possible. Specifically, we will synthesize polymers with absorption band ranging from 400 nm to beyond 1 μm with carrier mobilities higher than 10^{-4} cm^2/Vs. Polymer-fullerene (both $PC_{60}BM$ and $PC_{70}BM$ along with more recently developed derivatives) blend morphology will be optimized using different solvent/heat treatments as well as additives to the blends. The final device will be enhanced using anode and cathode interlayers to enhance carrier extraction to the electrodes. With the ability to synthesize broadly absorbing polymers, control the donor-acceptor phase morphology and engineer the device structure, it is expected that the power conversion efficiency of polymer solar cells can reach 10% at the end of the two-year program.

Summary of Progress

Extensive efforts have been directed at developing polymer bulk heterojunction (BHJ) solar cells because of their potential for low-cost energy harvesting. The device geometry of typical laboratory-scale polymer solar cells comprises a bottom indium tin oxide (ITO) anode, an anode interfacial layer, a photoactive layer and a low-work-function top metal cathode. Because vacuum deposition of low-work-function metals is required for these top cathode devices, it is not viable to use this device architecture in large-scale roll-to-roll (R2R) processing.

To avoid the low-work-function metals used in such devices, two strategies have been adopted. In the first, the low-work-function metal is replaced with a transition-metal oxide such as TiO_x or ZnO. In the second, the polarity of the BHJ devices is inverted. Specifically, these so-called 'inverted cells' have an oxide electron-transporting layer (ETL)-coated ITO as the bottom cathode and a screen-printed silver layer as the top anode; to date, this device architecture is prototypical for R2R processing. To fabricate the ETL, solution-processed metal oxides have been widely used in large-scale inverted solar cells to reduce the ITO work function. In particular, ZnO colloidal nanoparticles are used for the ETL because of their low work function, high electron mobility and optical transparency, as well as their ease of synthesis. However, the major challenges in using ZnO nanoparticle films as ETLs are the presence of defects with adsorbed oxygen and the poor spatial distribution of the nanoparticles over a large area. Accordingly, there is a need to develop low-defect and uniform ZnO films so as to realize high-efficiency inverted polymer solar cells.
Here, we report a new method for enhancing charge collection in inverted polymer BHJ solar cells using a ZnO–poly(vinyl pyrrolidone) (PVP) composite sol–gel film as the ETL, and demonstrate inverted polymer solar cells that operate with laboratory-measured PCEs in excess of 8% and certified efficiencies of 7.4% under AM 1.5G illumination at 100 mW cm^{-2}. The composite film, termed 'ZnO–PVP nanocomposite' for clarity, consists of ZnO nanoclusters whose growth is mediated by a PVP polymeric matrix. ZnO–PVP nanocomposite films have been studied previously in relation to chemical/biosensing applications and have the following advantages over conventional ZnO sol–gel films. First, the ZnO nanocluster size and its concentration can be tuned by controlling the Zn^{2+}/PVP ratio. Second, the distribution of ZnO nanoclusters in the PVP polymer is uniform compared to the aggregation observed in ZnO sol–gel films without PVP. We hypothesized that inverted solar cells using this composite would demonstrate enhanced device performance. Furthermore, because the sol–gel processing for the ZnO–PVP nanocomposite is performed in air, this approach to depositing the ZnO ETLs is compatible with large-scale R2R processes.

We recently reported the synthesis and BHJ solar cell performance of a dithienogermole (DTG) containing an alternating conjugated donor–acceptor polymer, in which N-octylthienopyrrolodione (TPD) was used as the acceptor. Inverted polydithienogermole-thienopyrrolodione (PDTG-TPD):[6,6]-phenyl-C71-butyric acid methyl ester ($PC_{71}BM$) solar cells demonstrated a higher short-circuit current density (J_{sc}) and fill factor (FF) than devices with an analogous polydithienosilole-containing polymer (PDTS–TPD), leading to inverted polymer solar cells with PCEs of 7.3%. To determine whether our ZnO–PVP nanocomposite films would enhance charge collection for inverted solar cells, we fabricated inverted PDTG–TPD:$PC_{71}BM$ BHJ solar cells using the nanocomposite as an ETL.

Progress Report

The photo J–V characteristics for inverted PDTG–TPD:$PC_{71}BM$ solar cells were measured under AM 1.5G solar illumination at 100 mW cm^{-2}. The photovoltaic (PV) performance results for the inverted cells with ZnO–PVP nanocomposites are shown in Figure 1. On initial light exposure the inverted solar cells had a low FF of 25.5% and J_{sc} of 10.9 mA cm^{-2}. With continuous illumination, device performance was enhanced significantly over time. After 10 min of light soaking, an enhanced FF of 63.7% and J_{sc} of 12.9 mA cm^{-2} were obtained, resulting in an average PCE of 7.0%. Previously, we reported inverted PDTG–TPD-based polymer solar cells with a FF of 68% using colloidal ZnO nanoparticlesas the ETL. We suspected that by using ZnO-PVP composite as the ETL, the ZnO-PVP surface would be compositionally rich in PVP, creating a contact barrier between the ZnO nanoclusters and $PC_{71}BM$ leading to the lower FF of our present devices.

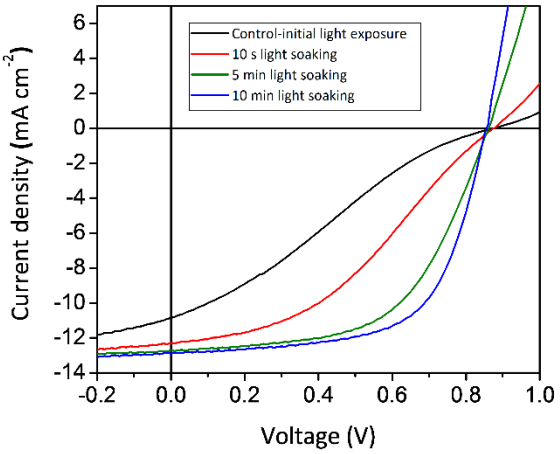

Figure 1. Effect of light soaking on device performance for inverted solar cells with as-prepared ZnO-PVP nanocomposite ETL.

To ensure a good contact between the ZnO nanoclusters and $PC_{71}BM$, we performed UV-ozone treatment on the ZnO–PVP nanocomposite films to remove PVP from the surface. Previous work has shown that UV-ozone treatment can remove PVP on colloidal nanoparticle film surfaces34. The removal of PVP did not alter the size, shape or distribution of the nanoclusters in the films. Based on these findings, we believed that the UV-ozone treatment would improve electronic coupling between the photo-active layer and the ZnO nanoclusters. The photo J–V characteristics for the inverted PDTG–TPD:$PC_{71}BM$ solar cells with UV-ozone treated ZnO–PVP nanocomposites are shown in Fig. 2a. All devices were tested under initial light exposure, and no additional light soaking was applied to the devices. The ZnO–PVP nanocomposite films were UV-ozone treated for 5, 10, 20 and 30 min, leading to significant enhancements in the J_{sc} and FF values for the inverted PDTG–TPD:$PC_{71}BM$ solar cells compared to cells with as-prepared nanocomposite films. Table 1 summarizes the device performance for inverted solar cells with treated ZnO–PVP nanocomposite films. UV-ozone treating the ZnO–PVP nanocomposite films for 10 min led to an optimal device with enhancements in both J_{sc} and FF compared to the light-soaked devices without UV-ozone treatment, and resulting in an average PCE of 8.1%. This average PCE of 8.1+0.4% is based on measurements from 102 fabricated solar cells. Our best device had a J_{sc} of 14.4 mA cm^{-2}, V_{oc} of 0.86 V, FF

of 68.8% and PCE of 8.5%. For devices with ZnO–PVP nanocomposite films that had been UV-ozone treated for less than or more than 10 min, a reduction in FF was observed. For the shorter treatment, we attribute this reduction in FF to incomplete removal of the PVP from the surface of the composite film. For the longer treatment, excess oxygen is present on the ZnO film surface, which reduces the electron extraction efficiency. Based on these findings, we conclude that removal of extra PVP from the ZnO–PVP nanocomposite film surface by UV-ozone treatment greatly enhances the charge collection efficiency of these devices.

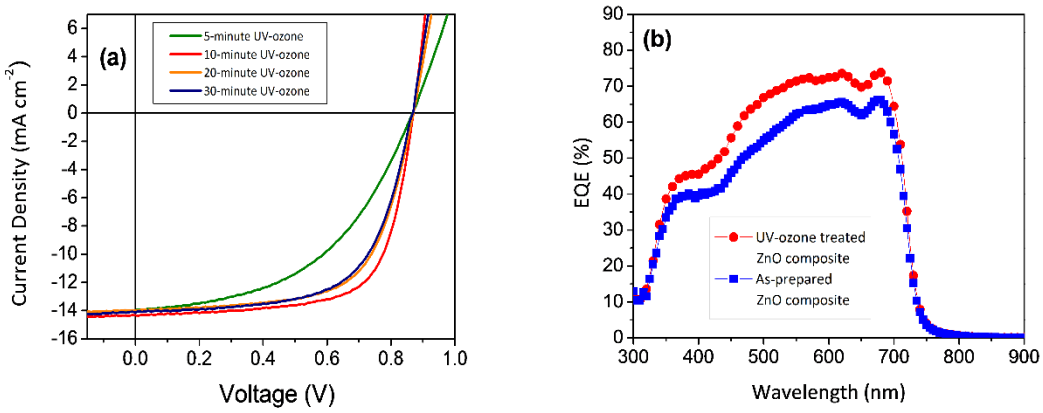

Figure 2. (a) Photo J-V curves of inverted PDTG-TPD:$PC_{71}BM$ solar cells with UV-ozone treated ZnO-PVP nanocomposite films as ETLs for various treatment times (5, 10, 20, 30 min) under initial AM 1.5G solar illumination at 100 mW cm^{-2}. (b) Corresponding EQE for the devices with as-prepared and 10 min UV-ozone treated ZnO-PVP nanocomposite films.

To confirm the accuracy of the photo J–V measurements, the external quantum efficiency (EQE) spectra for the solar cells with as-prepared and 10 min UV-ozone treated ZnO–PVP nanocomposite films were measured; these are compared in Fig. 2b. An enhanced efficiency is observed throughout the full spectral range from 350–700 nm for cells with UV-ozone treated ZnO–PVP nanocomposite films when compared to cells without UV-ozone treatment. The maximum EQE for the optimized inverted PDTG–TPD:$PC_{71}BM$ solar cell with UV-ozone treated nanocomposite films was 73.6%. The J_{sc} value was then calculated by integrating the EQE data with the AM 1.5G spectrum. The calculated J_{sc} value of 14.5 mA cm^{-2} is in good agreement with the directly measured J_{sc} value.

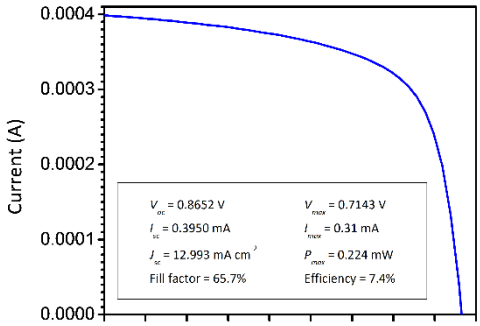

Figure 3. Certified I-V characteristics for an inverted PDTG-TPD:$PC_{71}BM$ solar cell with 10 min UV-ozone treated ZnO-PVP nanocomposite ETL.

Encapsulated devices with UV-ozone treated ZnO–PVP nanocomposite films were then sent to NEWPORT Corporation for certification. The photo J–V characteristics and the corresponding solar cell parameters are shown in Figure 3. A PCE of 7.4+0.2% was certified for the devices. Although this certified efficiency is 9% less than that measured in our laboratory because of a reduction in J_{sc} and FF in the certified device, we attribute the reduction in PCE in the certified cells to degradation because of a non-optimized encapsulation process. The devices were retested in our laboratory after certification and we obtained an efficiency (7.2%) comparable to the certified results.

The enhanced device performance with UV-ozone treated ZnO–PVP nanocomposite films is believed to be attributable to the modified surface composition promoting charge collection. The nanoscale surface morphologies of the as-prepared and UV-ozone treated ZnO–PVP nanocomposite films were investigated by atomic force microscopy (AFM). Figure 4a,b shows the threedimensional surface topography images

for the nanocomposite film before and after UV-ozone treatment. The ZnO–PVP nanocomposite film shows an increase in r.m.s. roughness from 7.07 nm to 9.18 nm following UV-ozone treatment, suggesting that PVP is removed with this treatment, leaving the ZnO nanoclusters exposed at the surface. This removal of the PVP is more clearly shown in the AFM phase images in Figure 4c,d. For the nanocomposite film without UV-ozone treatment, no nanoclusters can be observed, indicating that the surface is covered by a thin layer of PVP. However, the phase image for the UV-ozone treated ZnO–PVP nanocomposite film shows that the PVP domain size has been reduced to 50–100 nm and that the ZnO nanoclusters are now exposed on the surface. The PVP-rich and ZnO nanocluster rich surfaces of the nanocomposite films before and after UVozone treatment, respectively, are shown schematically in Figure 4e,f. This change in surface morphology from being PVP-rich before UV-ozone treatment to ZnO-rich after treatment supports our idea that the removal of PVP from the nanocomposite film by UV-ozone treatment leads to improved charge collection in our inverted polymer solar cells due to better electronic coupling between the ZnO nanoclusters within the nanocomposite film and $PC_{71}BM$ in the active layer.

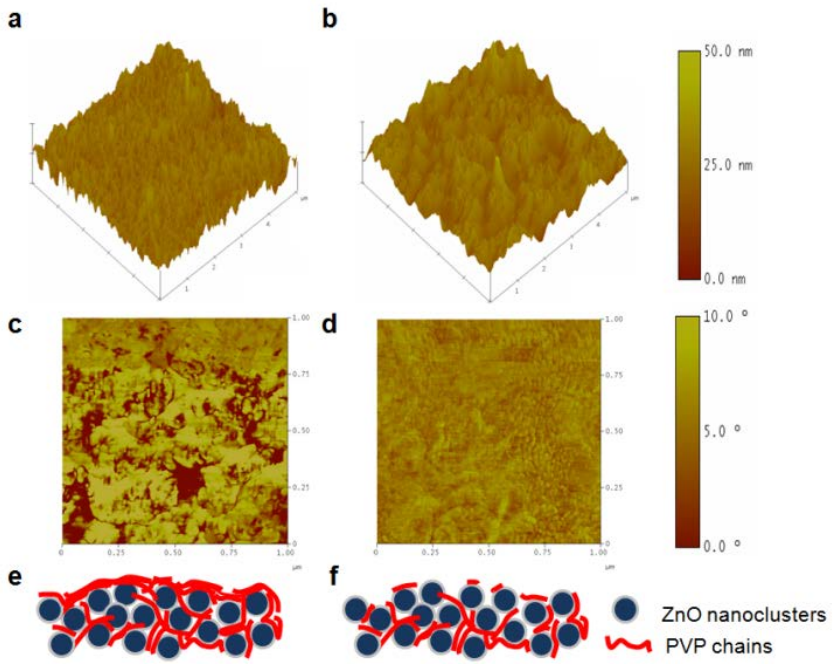

Figure 4. AFM images of a ZnO-polymer composite film before and after surface modification. (a), (c), and (e) shows the 3-D topography, phase image, and the schematic image for the composite film before surface treatment. (b), (d), and (f) shows the 3-D topography, phase image and schematic image for the same film after treatment.

To further confirm that the compositional changes determined from the AFM data were due to the removal of PVP, X-ray photoemission spectroscopy (XPS) was performed on the ZnO–PVP nanocomposite films. Considering the period of UV-ozone treatment required to optimize device performance, it is believed that some changes in the chemical composition of the ZnO might be plausible. The core-level XPS spectra for C 1s, O 1s and Zn 2p were measured for the as-prepared and 10 min UV-ozone treated ZnO–PVP nanocomposite films. The binding energies were calibrated by taking the C 1s peak (284.6 eV) as a reference. The O 1s XPS spectra for as-prepared and UV-ozone treated ZnO–PVP nanocomposite films are shown in Figure 5a. UV-ozone treatment increased the relative magnitude of the peak at 531.4 eV (corresponding to the oxygen atoms bonded to the zinc in the ZnO matrix) by 37%. Thus the number of Zn–O bonds in the wurtzite structure of ZnO at the surface of the film is increased. UV-ozone treatment also increased the relative magnitude of the peak at 530.0 eV, which corresponds to O^{2-} ions present in the porous ZnO clusters, but not chemically bonded to zinc in the ZnO wurtzite structure. Figure 5b shows the

Zn 2*p*3/2 XPS spectra for the as-prepared and UV-ozone treated ZnO–PVP nanocomposite films. The intensity of the peak at 1,021.6 eV, which corresponds to the Zn–O bonds, increases after UV-ozone treatment. These results are in agreement with the result for the O 1s XPS spectra. Based on the O 1s and Zn 2p XPS spectra, we conclude that the chemical composition of the ZnO nanoclusters on the surface of the nanocomposite film has become oxygen-rich after UV-ozone treatment.

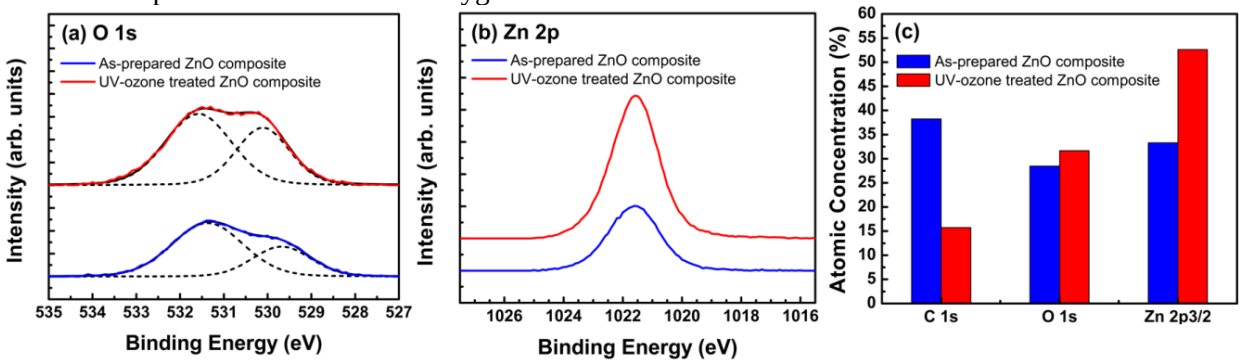

Figure 5. XPS data for the as-prepared and 10 min UV-ozone treated ZnO-polymer composite films. (a) O 1s and (b) Zn 2p XPS spectra for the composite films. (c) Atomic concentrations of carbon, zinc, and oxygen before and after UV-ozone treatment based on the corresponding XPS spectra.

The atomic concentrations of carbon, oxygen and zinc in the as-prepared and 10 min UV-ozone treated ZnO–PVP nanocomposite films based on the C 1s, O 1s and Zn 2p XPS spectra are summarized in Figure 5c. The atomic concentration of carbon from the PVP in the nanocomposite is significantly reduced by UV-ozone treatment (from 38.2% to 15.7%). Conversely, the atomic concentrations of oxygen and zinc present in the nanocomposite film both increase from 28.5% and 33.3% for the untreated film to 31.6% and 52.6%, respectively, for the treated film. The relatively smaller increase in oxygen atomic concentration compared to zinc is due to the competition between the increases in oxygen content arising from UV-ozone treatment and the decrease in oxygen content coming from the removal of PVP. These results strongly support our assertion that UV-ozone treatment removes PVP from the surface of the ZnO–PVP nanocomposite film.

To conclude, improved charge collection efficiency has been demonstrated in inverted PDTG–TPD BHJ solar cells using a UV-ozone treated ZnO–PVP nanocomposite film as the ETL to obtain organic polymer solar cells with PCEs in excess of 8% under AM 1.5G illumination at 100 mW cm^{-2}. The use of PVP as an organic capping molecule and polymeric matrix for ZnO produced electron-transporting nanocomposite films, which had excellent film-forming characteristics. We found that UV-ozone treatment was required to remove PVP from the surface of the film, and consequently exposed the ZnO nanoclusters to the film charge collection by the nanocomposite film.